**Discovery of 14*S*-(2'-chloro-4'-nitrophenoxy)-8*R/S*,17-epoxy andrographolide as EV-A71 infection inhibitor**

Kun Dai[a,1], Jie Kai Tan[b,1], Weiyi Qian[a], Regina Ching Hua Lee[b], Justin Jang Hann Chu[b, c, d], Guo-Chun Zhou[a]


[a] School of Pharmaceutical Sciences, Nanjing Tech University, Nanjing, Jiangsu, China
[b] Laboratory of Molecular RNA Virology and Antiviral Strategies, Department of Microbiology and Immunology, Yong Loo Lin School of Medicine, National University of Singapore, 117545 Singapore, Singapore
[c] Infectious Disease Translational Research Programme, Yong Loo Lin School of Medicine, National University of Singapore, 117597 Singapore, Singapore
[d] Collaborative and Translation Unit for HFMD, Institute of Molecular and Cell Biology, Agency for Science, Technology and Research, 138673 Singapore, Singapore

* Corresponding authors at: School of Pharmaceutical Sciences, Nanjing Tech University, Nanjing, Jiangsu, China (G.-C. Zhou). Laboratory of Molecular RNA Virology and Antiviral Strategies, Department of Microbiology and Immunology, Yong Loo Lin School of Medicine, National University of Singapore, 117545 Singapore, Singapore (J.J.H. Chu).

E-mail addresses: miccjh@nus.edu.sg (J.J. Hann Chu), gczhou@njtech.edu.cn (G.-C. Zhou).

[1] These authors contributed equally to the work.

**Abstract**

Human enterovirus A71 (EV-A71) is a major etiological agent of hand-foot-and-mouth disease (HFMD) and there is presently no internationally approved antiviral against EV-A71. In this study, it is disclosed that 14*S*-(2'-chloro-4'-nitrophenoxy)-8*R*/*S*,17-epoxy andrographolide (**2**) was discovered to be an effective inhibitor against EV-A71 infection showing significant reduction of viral titre. In addition to EV-A71, compound **2** exerts broad-spectrum antiviral effects against other enteroviruses. It is revealed that compound **2** inhibits the post-entry stages of EV-A71 viral replication cycle and significantly reduces viral protein expression of structural proteins such as VP0 and VP2 via inhibiting EV-A71 RNA replication. Moreover, the inhibitory property of compound **2** is specific to viral RNA replication. Furthermore, compound **2** is more likely to target a host factor in EV-A71 RNA replication. As a result, introduction of epoxide at positions 8 and 17 of andrographolide is effective for anti-EV-A71 infection and is a potential anti-EV-A71 strategy. Further work to discover more potent andrographolide derivatives and elucidate comprehensive SAR is under way.

**Keywords:** Human enterovirus A71; Andrographolide; Epoxide; Viral RNA replication; Targeting host factor; Broad-spectrum anti-enterovirus agent

## 1. Introduction

Human enterovirus A71 (EV-A71) is a major etiological pathogen of hand-foot-and-mouth disease (HFMD). It belongs to the virus family *Picornaviridae*, the genus *Enterovirus* and the species *Enterovirus A*. The virus was first discovered from a 9-month-old infant diagnosed with encephalitis in California, USA, in 1969 [1]. It then spread to Europe with outbreaks occurring in Bulgaria in 1975 [2] and Hungary in 1978 [3]. Since then, EV-A71 has mainly been epidemic in the Asia-Pacific region and causing recurring outbreaks in Australia, Cambodia, China mainland, Japan, Malaysia, South Korea, Singapore, Thailand, Taiwan and Vietnam [4]. Notably, China mainland recorded 13.7 million cases from 2008 through 2015, which included 123,261 severe cases and 3,322 deaths [5].

EV-A71 can be transmitted through physical contact, respiratory secretions and faeces from an infected individual [6, 7]. When exposed to EV-A71, the virus can infect tissues in the digestive and respiratory tracts namely the tonsillar crypt epithelium and replicate [8]. Following replication, the virus can then spread from the skeletal muscle to the central nervous system through the peripheral nerves which can affect the brain and spinal cord, resulting in serious neurological complications [8]. While EV-A71 infections are largely asymptomatic, the virus can cause HFMD among young children [4]. HFMD is a self-limiting disease with symptoms manifesting as fever, mouth ulcers and skin rash on the palms of the hands and soles of the feet [4]. In severe cases, the infection can result in serious neurological conditions like acute flaccid paralysis, aseptic meningitis and brainstem encephalitis, resulting in cognitive and neurodevelopmental impairment [9].

Presently, there is no internationally approved antiviral or vaccine against EV-A71. Although China has developed and approved vaccines against EV-A71 C4a strain,

the applicability of these vaccines against other strains have yet to be proven for worldwide use [10]. Also, experimental antiviral agents like pleconaril and ribavirin have contradicting reports on their in vitro and in vivo antiviral activity against EV-A71 [11-13]. As such, severe EV-A71 infections are still primarily managed by supportive treatments to prevent cardiopulmonary failure and improve clinical outcome [14]. To control EV-A71 outbreaks, existing measures include public health surveillance and prevention of transmission by handwashing and avoiding contact with infected individuals [15]. However, with the rise of EV-A71 outbreaks across the world in the last decade and considering the possible neurological complications involved with the viral infection, there is a pressing need to devise a safe and effective antiviral treatment to combat future outbreaks.

Andrographolide (**1**, abbreviated as andro, Scheme 1) [16-21] is a bicyclic diterpenoid lactone and one of major components isolated from *Andrographis paniculata* [Burm. F.] Nees, which is known as a "natural antibiotic" commonly used in China, India and Southeast Asia to reduce inflammation and "heat-clearing and detoxifying" defined in Chinese medicines. Andro can exert as a promising drug targeting multi-symptoms [22-25] and was demonstrated as NF-κB modulator [26] and Keap1-Nrf2-HO-1 signal pathway activator [27-30] by covalent binding. Andro and its concomitant diterpenes from *Andrographis paniculata* (Burm. F) Nees and their derivatives have discovered antiviral activity [23, 24, 31, 32]. As andro has poor oral bioavailability [33] which limits its clinical application, modification of andro has become an attracting field [34-36]. Importantly, active derivatives of andrographolide of "Xiyanping", "Chuanhuning", "Yanhuning", and "Lianbizhi" have been used in China to treat bacterial and viral infections for many years [37-40]. Moreover, "Xiyanping", as andro sulfonate complex, is a moderate anti-HFMD agent and has been used to clinically treat HFMD [41-43]. These results inspired us to explore more potent anti-HFMD analogs of andro by novel and effective modification to prevent HFMD from spreading to meet urgent need of anti-HFMD treatment. In this study, 14$S$-(2'-chloro-4'-nitrophenoxy)-8$R$/$S$,17-epoxy andrographolide (**2**) was discovered as an effective anti-EV-A71 agent. Here, we report the discovery and action of mode of compound **2** against EV-A71 infection.

## 2. Materials and methods
### 2.1. Synthesis of **2** and **6**
Synthesis of epoxy andrographolide analogs of **2** and **6** is shown in Scheme 1 (upper and right panel). According to previously reported methods [44-47], starting from andrographolide (Nanjing Chemlin Chemical Industry Co., Ltd., Nanjing, China), 3,19-acetonylidene andrographolide (**3**) was yielded and then 14β-aryloxy andrographolide **4** were afforded by Mitsunobu reaction. After deprotection of 3,19-acetonylidene from **4** by 4-methylbenzenesulfonic acid monohydrate (TsOH·$H_2O$) gave the intermediate **5** in 87.0% yield, epoxidation [48-50] of 8,17-olefin of **5** by 3-chloroperbenzoic acid (mCPBA) was conducted in dichloromethane (DCM) to form 8,17-epoxide **2** (total yield of 86.1%) which includes two inseparable isomers of 8$R$,17-epoxide **2a** (20% α-epoxide, minor) and 8$S$,17-epoxide **2b** (80% β-epoxide, major) by thin layer chromatography (TLC) and silica gel column chromatography. Acetylation

of compound **2** by acetyl chloride (AcCl) and triethylamine (TEA) yielded 19-acetylated product **6** containing two inseparable isomers of 19-acetoxy-8*R*,17-epoxide **6a** (15% α-epoxide, minor) and 19-acetoxy-8*S*,17-epoxide **6b** (85% β-epoxide, major) in total yield of 73.2%. Compared with the ratio of **2a** in compound **2**, slightly lower ratio of **6a** in compound **6** may be due to loss in separation process or/and ignored incomplete reaction of **2a**.

Isomer ratios of 8*R*,17-epoxide **2a**/8*S*,17-epoxide **2b**, and 19-acetoxy-8*R*,17-epoxide **6a**/19-acetoxy-8*S*,17-epoxide **6b** were determined by ^{1}H NMR and HPLC analysis.

*2.2. Synthesis of stereo-pure isomers of 2b*

In order to identify two isomers of **2a** and **2b** in compound **2**, stereo-pure isomer of **2b** was synthesized as following route (Scheme 1, left bottom panel) based on known stereo-selective incorporation [48-50] of 8*S*,17-epoxide. Briefly, direct epoxidation of andro (**1**) afforded 8*S*,17-epoxide **7** [23a], and then protection of **7** by 2,2-dimethoxypropane in DCM and catalysed by pyridinium *p*-toluenesulfonate (PPTS) provided 3,19-acetonylidene 8*S*,17-epoxide **8** [23b]. Both structures of **7** and **8** were confirmed by single crystal X-ray diffraction analysis (CCDC IDs 631,560 [23a] and 953,258 [23b], respectively). At last, Mitsunobu reaction by triphenylphosphine (PPh$_3$) and diisopropyl azodicarboxylate (DIAD) in tetrahydrofuran (THF) of pure β-epoxide isomer **8** provided key intermediate **9**, and formation of pure 8*S*,17-epoxide isomer **2b** was fulfilled by deprotection of 3,19-acetonylidene from **9** by TsOH·H$_2$O in methanol.

With stereo-pure 8*S*-epoxide isomer **2b**, assignments of **2a** and **2b** in **2** and **6a** and **6b** in **6** become reliable that 8*S*,17-epoxide isomers of **2b** and **6b** are major isomers in compound **2** and compound **6** as predicted, respectively. Comparison of compound **2** with stereo-pure 8*S*,17-epoxide isomer **2b** was determined by ^{1}H NMR and HPLC.

*2.3. Cells, viruses and compounds preparation*

Human muscle rhabdomyosarcoma cells (RD) (CCL-136; ATCC, Manassas, USA) and African green monkey kidney cells (Vero) (CCL-81; ATCC, Manassas, USA) were exploited in this study. RD and Vero cells were cultivated in Dulbecco's Modified Eagle's Medium (DMEM; Sigma-Aldrich, St. Louis, USA) complemented with 10% heat-inactivated fetal calf serum (HI-FCS; Capricorn Scientific, Ebsdorfergrund, Germany) and supplemented with 2 g of sodium hydrogen carbonate (Sigma-Aldrich, St. Louis, USA). Both cell lines were cultured at 37 °C, 5% CO$_2$. EV-A71 strain 41 (Accession no. AF316321.2), Enterovirus D68 (EV-D68) (Accession No. KM851231), Coxsackievirus A6 (CV-A6) (Accession No. KC866983.1) and Coxsackievirus A16 (CV-A16) (Accession No. U05876) were exploited in this study. All viruses were expanded in RD cells in DMEM, 2% HI-FCS and incubated at 37 °C, 5% CO$_2$ except for EV-D68 (33 °C). All synthesised compounds were dissolved in 100% DMSO (Sigma-Aldrich, St. Louis, USA) to final concentrations of 10 mM.

### 2.4. Cell viability assay

Cell viability assay was performed to determine the cytotoxicity profile. RD cells were seeded on 96-well plates (Corning Inc., Corning, USA) at a seeding density of $2 \times 10^4$ cells per well and incubated at 37 °C, 5% $CO_2$ overnight. The cells were treated with varying concentrations of compound **2** diluted in DMEM, 2% HI-FCS and further incubated at 37 °C, 5% $CO_2$ for 12 h. Cells treated with 0.1% DMSO and DMEM, 2% HI-FCS functioned as vehicle and negative controls respectively. Following incubation, the compound was discarded and 100 µL of diluted alamarBlue™ Cell Viability Reagent (Thermo Fisher Scientific, Waltham, USA) (1:10 DMEM, 2% HI-FCS) was pipetted to each well. The plates were incubated at 37 °C, 5% $CO_2$ for 3 h. The fluorescence readings at emission and excitation wavelengths of 600 nm and 570 nm were then obtained by the Infinite™ 200 series microplate reader (Tecan). Fluorescence readings obtained from compound-treated and 0.1% DMSO-treated cells were normalised against the negative controls to measure the relative cell viability. All experiments were performed in triplicates.

### 2.5. Dose-dependent inhibition assay

Dose-dependent inhibition assay was performed to determine the inhibitory profile. RD cells were seeded on 24-well plates (Greiner Bio-One, Kremsmünster, Austria) at a seeding density of $1.5 \times 10^5$ cells per well and incubated overnight. The cells were then infected with 100 µL of EV-A71 at MOI (multiplicity of infection) of 1 for 1 h at 37 °C, 5% $CO_2$. After infection, the cells were washed twice with 1 mL of phosphate buffered saline (PBS) and treated with 1 mL of compound **2**, at varied concentrations diluted in DMEM, 2% HI-FCS. The treated EV-A71-infected cells were further incubated at 37 °C, 5% $CO_2$ for 12 h. Following incubation, the plates were subjected to 2 cycles of freeze-thawing (-80 °C; 37 °C) before recovering the supernatant for viral plaque assay to ascertain the viral titre. All experiments were performed in triplicates.

### 2.6. Viral plaque assays

Viral titres were ascertained by viral plaque assays. For plaque assays involving EV-A71 and other *Enteroviruses* (EV-D68, CV-A6, CV-A16), RD cells were seeded on 24-well plates at a seeding density of $2.4 \times 10^5$ cells per well and incubated at 37 °C, 5% $CO_2$ overnight. Supernatants collected from the virus-infected samples were diluted serially in DMEM, 2% HI-FCS from dilution factors of $10^{-1}$ to $10^{-7}$. The seeded cells were infected with 100 µL of various diluted virus suspensions and incubated at 37 °C, 5% $CO_2$ (33 °C for EV-D68) for 1 h. Following viral adsorption, the cells were washed twice with 1 mL of PBS before the addition of 1 mL overlay medium comprising DMEM, 2% HI-FCS and 0.5% agarose (Vivantis, Shah Alam, Malaysia). Plates with EV-A71, EV-D68, CV-A6, CV-A16 supernatants were incubated for 4 days for plaque formations. The plates were subsequently fixed and stained with 4% paraformaldehyde and 1% crystal violet (Sigma-Aldrich, St. Louis, USA) overnight. Viral plaques formed were manually counted to determine the viral titre in PFU/mL.

### 2.7. Time-of-addition and time-of-removal assays

208    For both time-of-addition and time-of-removal assays, RD cells were seeded on
209  96-well plates at a seeding density of $2 \times 10^4$ cells per well and incubated overnight.
210  The cells were then infected with EV-A71 at MOI of 1 for 1 h and washed twice with
211  100 μL of PBS. For time-of-addition assay, each well was topped up with 100 μL of
212  DMEM, 2% HI-FCS and at time-points of 0, 0.5, 1, 2, 4, 6, 8, 10 h post infection (hpi),
213  the media was discarded and 100 μL of 10 μM of compound **2**, diluted in DMEM, 2%
214  HI-FCS, was added. For time-of-removal assay, each well was treated with 100 μL of
215  10 μM of compound **2** and at time-points of 0, 0.5, 1, 2, 4, 6, 8, 10 hpi, the compound
216  was discarded and topped up with 100 μL of DMEM, 2% HI-FCS. At 12 hpi, all plates
217  were frozen down for viral plaque assay. All experiments were performed in triplicates.
218
219  *2.8. Pre-treatment assay*
220    RD cells were seeded on a 24-well plate at a seeding density of $1.5 \times 10^5$ cells
221  per well and incubated overnight. The cells were treated with 250 μL of 0.1% DMSO
222  or varying concentrations of compound **2** and incubated at 37 °C, 5% $CO_2$ for 2 h.
223  Following incubation, the cells were washed twice with 100 μL of PBS. Each well was
224  then infected with 100 μL of EV-A71 at MOI of 1, incubated at 37 °C, 5% $CO_2$ for 1 h
225  and washed twice with 100 μL of PBS. Each well was then topped up with 1 mL of
226  DMEM, 2% HI-FCS and incubated at 37 °C, 5% $CO_2$ for 12 h. At 12 hpi, the plate was
227  frozen down for viral plaque assay. All experiments were performed in triplicates.
228
229  *2.9. Co-treatment assay*
230    RD cells were seeded on a 24-well plate at a seeding density of $1.5 \times 10^5$ cells
231  per well and incubated overnight. 500 μL of EV-A71 at MOI of 1 was treated with
232  500 μL of 10 μM of compound **2** or 0.1% DMSO and incubated at 37 °C for 30 min.
233  After which, the treated viruses were filtered centrifugally with a 100,000-molecular-
234  weight centrifugal filter unit (Sartorius, Göttingen, Germany) at 1,500 × g, 4 °C for
235  5 min to remove unbound compound and DMSO molecules. The treated viruses were
236  washed with 1 mL of PBS, filtered again at 1,500 × g, 4 °C for 5 min and then re-
237  suspended in 500 μL of DMEM, 2% HI-FCS. After which, the seeded cells were
238  infected with 100 μL of the treated viruses, incubated at 37 °C, 5% $CO_2$ for 1 h and
239  washed with 100 μL of PBS twice. Each well was then added with 1 mL of DMEM, 2%
240  HI-FCS and incubated at 37 °C, 5% $CO_2$ for 12 h. At 12 hpi, the plate was frozen down
241  for viral plaque assay. All experiments were performed in triplicates.
242
243  *2.10.  Entry bypass assay*
244    RD cells were seeded on a 24-well plate at a seeding density of $1.5 \times 10^5$ cells
245  per well and incubated overnight. EV-A71 viral RNA was extracted with QIAamp Viral
246  RNA Mini Kit (QIAGEN, Hilden, Germany). EV-A71 was first lysed with viral lysis buffer
247  and then precipitated with 100% ethanol. The nucleic acids were then dispensed into
248  the spin column, washed thrice with the washing buffers provided and then eluted with
249  50 μL of elution buffer. 500 ng of EV-A71 RNA and 1 μL of DharmaFECT 1
250  transfection reagent (Thermo Fisher Scientific, Waltham, USA) were mixed into 50 μL
251  of serum-free DMEM independently and incubated at room temperature for 5 min.
252  After which, both suspensions were combined and incubated at room temperature for
253  20 min to form transfection complexes. 100 μL of EV-A71 RNA-DharmaFECT 1

254  transfection complexes was then pipetted to the seeded RD cells and incubated at
255  37 °C, 5% $CO_2$ for 1 h for transfection to proceed. Following incubation, each well was
256  topped up with 400 µL of compound **2** or DMSO to make up the final desired
257  concentrations and incubated at 37 °C, 5% $CO_2$ for 12 h. At 12 hpi, the plate was
258  frozen down for viral plaque assay. All experiments were performed in triplicates.
259
260  *2.11.  SDS-PAGE and Western blot*
261      RD cells were seeded on a 24-well plate at a seeding density of $1.5 \times 10^5$ cells
262  per well and incubated overnight. The cells were either infected with 100 µL of EV-
263  A71 at MOI of 1 or mock-infected with 100 µL of DMEM, 2% HI-FCS for 1 h at 37 °C,
264  5% $CO_2$. After infection, the cells were washed twice with 1 mL of PBS before treating
265  with varying concentrations of compound **2** for 6 h at 37 °C, 5% $CO_2$. Cells treated
266  with 0.1% DMSO were used as vehicle controls. After 6 h, the compound was
267  discarded and 100 µL of 1x Laemmli buffer was pipetted to each well to lyse the cells.
268  The wells were scraped and the cell lysate was recovered and stored at −80 °C. To
269  separate the proteins in the cell lysate, the sample was first denatured at 100 °C for
270  10 min. 20 µL of the sample was loaded onto a 10% acrylamide gel which was ran at
271  100 V for 2.5 h. 4 µL of the Bio Basic 10–250 kDa Protein Ladder BZ0011G (Bio Basic,
272  Markham, Canada) was used as a molecular-weight size marker. Separated protein
273  bands on the gel were then transferred onto an activated polyvinylidene difluoride
274  (PVDF) membrane by operating the Trans-Blot Turbo system (Bio-Rad) at 1.3A for
275  10 min.
276
277      After which, the PVDF membrane was first blocked with 2% bovine serum
278  albumin (BSA; Sigma Aldrich, St. Louis, USA) dissolved in Tris-buffered saline-Tween
279  20 (TBST) for 30 min. After blocking, the membrane was incubated with diluted mouse
280  anti-EV-A71 VP2 1° antibody, MAB979 (Merck Millipore, Burlington, USA; 1:10000
281  blocking reagent) at 4 °C overnight. Subsequently, the membrane was washed thrice
282  with TBST for 5 min. After which, the membrane was incubated with
283  diluted horseradish peroxidase (HRP) conjugated goat anti-mouse IgG 2° antibody
284  (Thermo Fisher Scientific, Waltham, USA; 1:10000 blocking reagent) at room
285  temperature for 1 h. Following incubation, the membrane was again washed thrice
286  with TBST for 5 min and exposed to an enhanced chemiluminescent substrate,
287  Immobilon Western Chemiluminescent HRP substrate (Thermo Fisher Scientific,
288  Waltham, USA) for 3 min before viewing using the C-DiGit Chemiluminescence
289  Western Blot Scanner (LI-COR). To re-probe the membrane, Restore PLUS stripping
290  buffer (Thermo Fisher Scientific) was employed to remove the bound antibodies. A
291  similar method was used to detect the loading control, β-actin. The membrane was
292  first blocked and then incubated with mouse anti-β-actin 1° antibody (Merck Millipore,
293  Burlington, USA) and HRP-conjugated goat anti-mouse IgG 2° antibody (Thermo
294  Fisher Scientific, Waltham, USA) diluted in blocking reagent in 1:10000, at room
295  temperature for 45 min. The membrane was later washed and exposed to view the
296  protein bands. All experiments were performed in triplicates.
297
298  *2.12.  Nano-luciferase reporter assay*

RD cells were seeded on 96-well plates at a seeding density of $2 \times 10^4$ cells per well and incubated overnight. The cells were transfected with either EV-A71 replication-competent replicon or replication-defective replicon. P1 region in both replicons was substituted with the NanoLuc luciferase gene (Promega). The EV-A71 replication-defective replicon has 159 nucleotides deleted from the 3D region. 100 ng of the purified RNA transcripts of either replicon, together with 0.2 μL of DharmaFECT 1 transfection reagent, 20 μL of DMEM, serum-free and 80 μL of DMEM, 10% HI-FCS were added to each well and incubated for 4 h at 37 °C, 5% $CO_2$ for transfection. Following incubation, the cells were washed once with 100 μL of PBS before treating with 100 μL of 0.1% DMSO, varying concentrations of compound **2**, 1 mM guanidine hydrochloride (GuHCl, RNA replication inhibitor; Sigma Aldrich, St. Louis, USA) or 10 μg/mL cycloheximide (CHX, general translation inhibitor; Sigma Aldrich, St. Louis, USA) and incubated for 12 h at 37 °C, 5% $CO_2$ before luciferase detection using the Nano-Glo kit (Promega, Madison, USA). All experiments were performed in triplicates.

*2.13. Bicistronic luciferase reporter assay*

RD cells were seeded on a 96-well white plate at a seeding density of $2 \times 10^4$ cells per well and incubated overnight. The cells were transfected with the bicstronic luciferase reporter construct containing a human cytomegalovirus promoter (CMV promoter) and downstream EV-A71 strain 41 IRES flanked by *Renilla* luciferase (R Luc) and firefly luciferase (F Luc) genes. 200 ng of the bicistronic construct, 0.4 μL of jetPRIME transfection reagent (Polypus-transfection, Illkirch-Graffenstaden, France) and 9.6 μL of jetPRIME buffer (Polypus-transfection, Illkirch-Graffenstaden, France) were incubated together for 10 min at room temperature to form transfection complexes before 90 μL of DMEM, 2% HI-FCS was added to obtain a total volume of 100 μL to transfect each well. The cells were incubated for 12 h at 37 °C, 5% $CO_2$ for the uptake of the transfection complexes. Following incubation, the transfection mixture was removed and the transfected cells were treated with 100 μL of 0.1% DMSO, 5 μM of compound **2** or 25 μM of apigenin (Sigma Aldrich, St. Louis, USA) and incubated for a further 12 h at 37 °C, 5% $CO_2$ before luciferase detection using the Dual-Glo Luciferase Assay System (Promega, Madison, USA). All experiments were performed in triplicates.

*2.14. Generation of resistant mutant*

RD cells were first seeded on a 24-well plate at a seeding density of $1.5 \times 10^5$ cells per well and incubated overnight. The seeded cells were infected with 200 μL of EV-A71 at MOI of 1 for 1 h at 37 °C, 5% $CO_2$. After infection, 800 μL of compound **2** were pipetted to the infected cells to attain a final concentration of 10 μM and incubated at 37 °C, 5% $CO_2$ for 12 h. Wells treated with 0.1% DMSO and DMEM, 2% HI-FCS were used as vehicle and negative controls respectively. Subsequently, the supernatant was recovered and viral titre was ascertained by viral plaque assay. 200 μL of the supernatant was also used to infect another plate of similarly seeded RD cells and the process was repeated. Resistant mutants would be obtained when the viral titre for the compound **2**-treated become similar to that of the controls.

*2.15. Antiviral activity of compound **2** against other enteroviruses*

345     The potential antiviral activity of compound **2** on other *Enteroviruses* (EV-D68,
346 CV-A6, CV-A16) were also investigated with dose-dependent inhibition assay. All virus
347 infections were performed at MOI of 1. EV-D68-infected cells were treated for 12 h,
348 CV-A16-infected cells were treated for 16 h and CV-A6-infected cells were treated for
349 4 days. Additional cell viability assay was performed to determine the suitable less-
350 cytotoxic concentrations for dose-dependent inhibition assay with longer drug
351 treatment duration (>12 h). All experiments were performed in triplicates.

352 *2.16.  Statistical analysis*
353     One-way analysis of variance (ANOVA) was utilised to assess the statistical
354 significance of the data collected in this study. When compared to the controls,
355 samples that showed significant statistical differences (p-values < 0.05, 0.01 and
356 0.001) were then further examined with a Dunnett's post-test. When comparing
357 between two different samples, a two-tailed students' T-test was carried out instead to
358 assess the significance of data.

359

360 **3.  Results**
361 *3.1. Compound **2** acts as an effective anti-EV-A71 agent*
362     The inhibitory activity against EV-A71 infection was conducted by a dose-
363 dependent inhibition assay using 0.1% DMSO as the solvent control. As shown in Fig.
364 1 and Table 1, compound **2** exhibits good anti-EV-A71 activity while its cytotoxicity is
365 low. As shown in Table 1, viral titre reduction of compound **2** is significant at 5 µM (1.6
366 $\log_{10}$ PFU/mL decrease) and 10 µM (2.3 $\log_{10}$ PFU/mL decrease), revealing that
367 compound **2** is an effective anti-EV-A71 agent with $IC_{50}$ (50% effective concentration
368 against EV-A71 infection) value of 0.95 µM while $CC_{50}$ (50% toxic concentration to RD
369 cells) value of 11.64 µM and selectivity index (SI) is higher than 12. 8*S*,17-
370 Epoxide **2b** is the major isomer in compound **2**, however, pure 8*S*,17-epoxide **2b** is
371 less active than compound **2** against EV-A71 infection (Table 1) and no $IC_{50}$ value
372 for **2b** was produced, reasoning that (1) the minor isomer of 8*R*,17-epoxide **2a** is the
373 more active isomer in compound **2**, or/and (2) it is also possible to execute anti-EV-
374 A71 activity of compound **2** by optimal combination of **2a** and **2b**. Even though
375 compound **2** and compound **6** exhibit almost the same value of viral titre reduction at
376 10 µM, no $IC_{50}$ values for compound **6** could be generated while viral titre reduction of
377 compound **6** (Table 1) is more sharply varied from 0.63 $\log_{10}$ PFU/mL decrease at
378 5 µM to 2.27 $\log_{10}$ PFU/mL decrease at 10 µM than that of compound **2**. Therefore, in
379 this study compound **2** was subjected to downstream analysis to elucidate its mode of
380 action due to its favourable selectivity index and structural novelty.

381

382 *3.2. Compound **2** inhibits the post-entry stages of EV-A71 viral replication cycle*
383     Time-of-addition and time-of-removal assays [51] were carried out to identify the
384 time window in the EV-A71 viral cycle in which compound **2** acts on. RD cells were
385 first seeded and infected with EV-A71. For time-of-addition assay, compound **2** was
386 added to the infected cells at pre-determined time points (Fig. 2**A**) to examine at which
387 time point, the inhibition effect would be lost and the viral titre would increase. For
388 time-of-removal assay, compound **2** was removed from the infected cells at similar
389 pre-determined time points to examine at which time point, the inhibition effect would
390 not be lost and the viral titre would plateau. At 12 h post infection (hpi), all supernatants

were recovered and viral titres were ascertained. Using both assays, we can identify the time window in the EV-A71 viral cycle in which compound **2** acts on. For time-of-addition assay, the viral titre increased significantly only when the drug was added from 10 hpi onwards (Fig. 2**B**), whereas for time-of-removal assay, the viral titre decreased significantly between 0 and 4 hpi and then plateau from 4 hpi onwards (Fig. 2**C**). The two graphs intercept at about 8.5 hpi (Fig. 2**D**). With reference to the growth kinetics of EV-A71 [52], compound **2** is likely to act on post-entry stages of EV-A71 viral cycle like RNA replication, protein translation, package and viral release. However, since there was a notable 0.5 $\log_{10}$ PFU/mL decrease in viral titre at 0.5 hpi for time-of-removal assay, antiviral activity against entry stages like internalisation and uncoating were not ruled out. As such, pre-treatment, co-treatment and entry bypass assays were conducted to examine the inhibitory effect of compound **2** on the entry stages.

Pre-treatment assay was executed to investigate if compound **2** is capable of inhibiting viral entry into host cells by binding with the host cell surface receptors and blocking viral attachment for receptor-mediated endocytosis. RD cells were first treated with varying concentrations of **2** for 2 h and then infected with EV-A71 (Fig. 2**A**). Supernatant was recovered 12 hpi and the viral titre was ascertained with viral plaque assay. Other than the highest concentration used, treatment with compound **2** displayed viral titres similar to that of 0.1% DMSO (Fig. 2**E**). Furthermore, viral reduction at the highest concentration was not as pronounced as treatment post-infection. Pre-treatment with compound **2** at 10 µM led to 0.4 $\log_{10}$ PFU/mL decrease while post-treatment of that led to 2.3 $\log_{10}$ PFU/mL decrease as mentioned earlier. This suggests that the antiviral property of compound **2** is unlikely to be acting on the host surface receptors that would affect EV-A71 entry into the host cells and the minor reduction in viral titre at 10 µM is probably due to drug toxicity.

Co-treatment assay was conducted to investigate if compound **2** is capable of inhibiting viral entry into host cells by interacting with the surface proteins of the viruses and blocking viral attachment for receptor-mediated endocytosis. EV-A71 was first treated with compound **2** for 30 min before being used to infect RD cells (Fig. 2**A**). Supernatant was recovered 12 hpi and the viral titre was ascertained with viral plaque assay. Co-treatment with compound **2** displayed viral titre similar to that of 0.1% DMSO (Fig. 2**F**) suggests that the antiviral property of compound **2** is unlikely to be acting on the surface proteins of the viruses that would affect EV-A71 entry into the host cells. Taking the results from both pre-treatment and co-treatment assays together, it is unlikely that compound **2** inhibits viral attachment and entry into host cells.

Entry bypass assay was conducted to investigate if compound **2** is able to inhibit stages of EV-A71 replication cycle occurring after the release of viral RNA into the host cytoplasm such as RNA replication, protein translation, package and viral release. RD cells were first transfected with EV-A71 RNA and then treated with varying concentrations of compound **2** (Fig. 2**A**). Supernatant was recovered 12 hpi and the viral titre was ascertained with viral plaque assay. Treatment with compound **2** led to

437 significant viral reduction at 10 µM (2.5 log$_{10}$ PFU/mL decrease) (Fig. 2**G**). This
438 suggests that compound **2** is likely to be acting on the aforementioned post-entry
439 stages of EV-A71 replication cycle since transfection eliminated the early stages (entry,
440 uncoating and release of RNA genome into host cytosol) from the viral replication
441 cycle and treatment with compound **2** displayed significant inhibition.

443 *3.3. Compound **2** reduces viral protein expression by inhibiting EV-A71 RNA*
444 *replication only*

445 Western blot analysis was conducted to evaluate the effect of compound **2** on EV-
446 A71 viral protein expression. RD cells were seeded, infected with EV-A71 and then
447 treated with varied concentrations of compound **2** as well as 0.1% DMSO serving as
448 vehicle control. At 6 hpi, the supernatant containing compound **2** was discarded and
449 the cells were lysed. Cell lysate samples were subjected to SDS-PAGE and Western
450 blot. Treatment with compound **2** led to significant dose-dependent reduction in the
451 band intensities of VP2 (28 kDa), an EV-A71 structural protein as well as VP0 (36 kDa),
452 an incomplete processed viral polypeptide made up of VP2 and VP4 (8 kDa), another
453 EV-A71 structural protein [53]. VP2 band was detected for 0.1% DMSO but not for any
454 treatment by compound **2** (Fig. 3**A**). In contrast, VP0 band was detected after
455 treatment with compound **2** at 1 µM with a 2-folds reduction in band intensity when
456 compared with 0.1% DMSO when compared with 0.1% DMSO (Fig. 3**A-B**). No VP0
457 band was detected at higher concentrations of compound **2**. β-Actin was probed as a
458 loading control. These results suggest that compound **2** can affect viral protein
459 synthesis in host cells. Considering previous results from pre-treatment, co-treatment
460 and entry bypass assays, it is likely that compound **2** targets RNA replication, protein
461 translation or both, which led to decreased viral protein expression in compound-
462 treated host cells.

464 To investigate if compound **2** inhibits RNA replication, protein translation or both,
465 the cells were first transfected with either EV-A71 replication-competent replicons or
466 replication-defective replicons before treated with varied concentrations of
467 compound **2**. At 12 hpi, the level of luminescence was measured to detect the amount
468 of luciferase present. Since the replication-defective replicon has
469 159 nucleotides deleted from the 3D region and 3D protein functions as viral RNA-
470 dependent RNA polymerase [6b], the deletion would disable RNA replication (Fig. 3**C**).
471 As such, luciferase production in cells transfected with the replication-defective
472 replicon is only due to IRES-mediated translation of the transfected replicon. In
473 contrast, the replication-competent replicon can be replicated to form more copies for
474 translation. As such, luciferase production in cells transfected with the replication-
475 competent replicon is due to IRES-mediated translation of both the transfected
476 replicon and the replicated copies. With this understanding, a RNA replication-specific
477 inhibitor like GuHCl will reduce luciferase production in cells transfected with the
478 replication-competent replicon while a translation-specific inhibitor like CHX will
479 reduce luciferase production in cells transfected with either replicon. In this study,
480 GuHCl and CHX were used as functional positive controls. Treatment with
481 compound **2** displayed similar inhibitory profile as GuHCl, with significant dose-
482 dependent reduction in the amount of luciferase present in the cells transfected with

483  the replication-competent replicon but not with the replication-defective replicon (Fig.
484  3**D-E**). This suggests that the inhibitory property of compound **2** is likely to be specific
485  to viral RNA replication only.
486
487    To confirm that treatment with compound **2** does not affect IRES-mediated
488  translation, a bicistronic reporter assay was carried out as described previously [54].
489  The cells were first transfected with a bicistronic reporter construct consisting of
490  a human cytomegalovirus promoter (CMV promoter) and downstream EV-A71 strain
491  41 IRES flanked by *Renilla* luciferase (R Luc) and firefly luciferase (F Luc) genes (Fig.
492  3**F**). The expression of R Luc is driven by the cap-dependent CMV promoter while the
493  expression of F Luc is driven by the cap-independent EV-A71 strain 41 IRES. The
494  transfected cells were subsequently treated with compound **2** and respective
495  luciferase activities were measured. The efficiency of IRES-mediated translation was
496  represented by the ratio of F Luc to R Luc (F Luc/R Luc). Apigenin, a known EV-A71
497  IRES inhibitor [55], was used as the positive control. Treatment with compound **2** at
498  5 μM show no significant difference in IRES activity when compared with 0.1% DMSO
499  (Fig. 3**G**) further reiterates that the inhibitory property of compound **2** is specific to viral
500  RNA replication only.
501
502  *3.4. Compound **2** is likely to target a host factor in EV-A71 RNA replication*
503    Attempts were made to generate resistant mutants against compound **2**. This was
504  done by repeatedly passaging EV-A71, together with increasing concentrations of
505  compound **2**, in RD cells (Fig. 4**A**). From Passage 1 to Passage 20, when treated with
506  5 μM of compound **2**, the viral titre fluctuated before slowly increasing from Passage
507  15 onwards. At Passage 21, we increased concentration of compound **2** to 7.5 μM and
508  the viral titre starts to gradually decrease again. We subjected the supernatant
509  recovered from Passage 30 to dose-dependent inhibition assay and found that
510  compound **2** remains effective in inhibiting the treated virus in a dose-dependent
511  manner (Fig. 4**B**). As such, we believe that compound **2** is likely to be targeting a host
512  factor which increases the difficulty of generating resistant mutants.
513
514  *3.5. Compound **2** exhibits broad-spectrum antiviral effects against other enteroviruses*
515    Dose-dependent inhibition assay was performed on other enteroviruses and one
516  flavivirus to determine if compound **2** possesses broad-spectrum antiviral activity. The
517  enteroviruses being investigated were CV-A16, CV-A6 and EV-D68. Compound **2**, at
518  5 μM, was able to inhibit all the enteroviruses mentioned with significant reduction in
519  viral titre (Fig. 5). As shown in Table 2, compound **2** was more potent towards CV-A16
520  ($IC_{50}$ = 0.46 μM) compared to CV-A6 ($IC_{50}$ = 1.12 μM), EV-D68 ($IC_{50}$ = 1.59 μM) and
521  even EV-A71 ($IC_{50}$ = 0.95 μM).
522
523  4. Discussion
524    While EV-A71 infections are generally asymptomatic or mild, there are cases of
525  severe neurological complications such as acute flaccid paralysis, aseptic meningitis
526  and brainstem encephalitis associated with the infections. Coupled with the surge of
527  EV-A71 outbreaks across the world in the last decade as well as the lack of

528 internationally approved antivirals to combat these infections, there is a pressing need
529 to develop safe and effective antivirals against EV-A71.
530
531     Traditionally, andro has been used in Chinese medicine to treat HFMD. "Xiyanping",
532 an andro sulfonate analogs complex, is employed widely in China to treat HFMD with
533 clinical efficacy [42, 56]. Andro was also reportedly able to inhibit EV-D68 by inhibiting
534 acidification of virus-containing endosomes after receptor-mediated endocytosis
535 hence trapping the virus in endosomes which would eventually be phagocytosed and
536 killed [57]. To further improve the anti-HFMD efficacy of andro, more potent analogs
537 of andro have to be derived by novel chemical modification. In this study, we found
538 that among the series of 14-aryloxy andrographolide modified with the introduction of
539 8,17-epoxide, 14$S$-(2'-chloro-4'-nitrophenoxy)-8$R/S$,17-epoxy andrographolide **2** was
540 discovered as an effective anti-EV-A71 agent.
541
542     Compound **2** is made up of two inseparable isomers of 8$R$,17-epoxide **2a** as a
543 minor (~20%) and 8$S$,17- epoxide **2b** as a major (~80%). It was well tolerated by the
544 cells below 10 µM and was able to significantly reduce the viral titre of EV-A71 infected
545 RD cells at 5 µM and 10 µM. The $CC_{50}$ and $IC_{50}$ values of compound **2** were
546 determined to be 11.64 µM and 0.95 µM respectively, which yield a selectivity index
547 of > 12, showcasing strong anti-EV-A71 activity with low cytotoxicity. We also tested
548 the pure 8$S$,17-epoxide isomer **2b** in hand against EV-A71 and found that it is less
549 effective in reducing the EV-A71 infection despite being the major isomer in
550 compound **2**. This suggests that either the minor isomer of compound **2**, 8$R$,17-
551 epoxide **2a**, is the more active anti-EV-A71 agent by **2a**'s more favourable orientation
552 in interaction with its target/s or the anti-EV-A71 activity of compound **2** stems from
553 the optimal combination of **2a** and **2b**. Furthermore, it is found that 19-
554 acetylated **6** (with the close but lower α-epoxide/β-epoxide ratio to compound **2**)
555 decreases inhibitory activity to EV-A71, reasoning that the lower ratio of minor 8$R$,17-
556 isomer in compound **6** than in compound **2** perhaps affords less anti-EV-A71 activity;
557 or else 19-hydroxy of compound **2** is the key or 19-acetylation is not an suitable
558 modification for inhibitory activity to EV-A71. These inspire us in future study to work
559 on the synthesis of stereo-pure compound **2a** in that **2a** can elucidate more valuable
560 pharmacological information.
561
562     Since compound **2** is a novel derivative of andro with no previously reported
563 antiviral activity, it was subjected to mechanistic studies to elucidate its antiviral
564 mechanism. Time-of-addition and time-of-removal assays were first carried out to
565 identify the time window in the EV-A71 viral cycle in which compound **2** acts on [51].
566 Compound **2** was either added to or removed from the infected cells at predetermined
567 time points. For time-of-addition assay, we wanted to identify the time point in which
568 when the compound was added, had missed its time window for inhibition, resulting in
569 loss of antiviral effect and increase in viral titre. For time-of-removal assay, we wanted
570 to identify the time point in which sufficient amount of the compound was internalised
571 and retained in the infected cells such that even when the compound was removed,
572 antiviral effect was not lost and viral titre started to plateau. We found that the viral titre
573 started to plateau at 4 hpi for time-of-removal assay and increase at 8 hpi for time-of-

574 addition assay, suggesting that compound **2** is likely to act on the post-entry stages of
575 EV-A71 viral cycle with antiviral activity acting between 4 hpi to 8 hpi. These
576 observations were supported by the results of subsequent entry bypass assay, with
577 compound **2** being effective in reducing EV-A71 infection even after direct transfection
578 of EV-A71 viral RNA into RD cells. In contrast, pre-treatment and co-treatment with
579 compound **2** were not able to significantly reduce EV-A71 infection. These results
580 confirm that compound **2** does not exert its antiviral activity on EV-A71 viral
581 attachment and entry into host cells. According to previous characterisation studies on
582 the viral kinetics of EV-A71, viral RNA replication begins at 3 hpi and peaks between
583 6 hpi and 9 hpi while viral protein synthesis begins at 6 hpi and peaks at 9 hpi [52].
584 Hence, we speculate that compound **2** is targeting viral RNA replication, protein
585 translation or both. However, we do not rule out the potential antiviral activity of
586 compound **2** against the intermediary steps between viral entry and RNA release such
587 as endosome acidification and uncoating especially since andro was reportedly able
588 to inhibit EV-D68, another species of enterovirus, through this mode of action [57].
589
590   Through Western blot, we found that treatment with compound **2** led to dose-
591 dependent reduction in viral proteins levels (VP0 and VP2) in host cells at 6 hpi. This
592 result corroborates the findings from time-of-addition and time-of-removal assays that
593 compound **2** is plausibly targeting viral RNA replication, protein translation or both,
594 which led to decreased viral protein expression. To understand the effects of
595 compound **2** on these two intrinsically-linked processes, nano-luciferase reporter
596 assay utilising EV-A71 replicons was performed. The cells were transfected with either
597 EV-A71 replication-competent replicon or EV-A71 replication-defective replicon before
598 treatment with compound **2**. The replication-defection replicon contains a 159-
599 nucleotides deletion in the 3D region (encodes for viral RNA-dependent RNA
600 polymerase) that disables RNA replication. As such, luciferase production in cells
601 transfected with the replication defective replicon is due to IRES-mediated translation
602 of the transfected replicon only. In contrast, the replication-competent replicon can be
603 replicated to form more copies for translation. Hence, luciferase production in cells
604 transfected with the replication-competent replicon is due to IRES-mediated
605 translation of both the transfected replicon and the replicated copies. The functionality
606 of this assay was validated with two positive controls, guanidine hydrochloride (GuHCl),
607 a RNA-replication inhibitor [58], and cycloheximide (CHX), a general translation
608 inhibitor [59]. Treatment with compound **2**, like GuHCl, lowered luciferase production
609 in cells transfected with the replication-competent replicon, in a dose-dependent
610 manner but not in cells transfected with the replication-defective replicon. This
611 suggests that compound **2** reduces viral protein expression by inhibiting EV-A71 RNA
612 replication specifically. To confirm that compound **2** has no effect on IRES activity, we
613 transfected the cells with a bicistronic reporter construct consisting of a CMV promoter
614 and downstream EV-A71 strain 41 IRES flanked by R Luc and F Luc genes. R Luc
615 expression and F Luc expression are driven by cap-dependent CMV promoter and
616 cap-independent EV-A71 IRES respectively. As such, we can measure the efficiency
617 of IRES-mediated translation using the ratio F Luc to R Luc. Upon treatment of the
618 transfected cells with compound **2**, we found no significant difference when compared
619 with 0.1% DMSO. In contrast, cells treated with apigenin, a known EV-A71 IRES

620 inhibitor [55], showed a significant drop in IRES activity. This supports the finding that
621 compound **2** targets EV-A71 RNA replication specifically to reduce EV-A71 infection.
622
623     Attempts to generate resistant mutants against compound **2** were unsuccessful.
624 We serially passage the EV-A71 in RD cells with increasing concentrations of
625 compound **2** for 30 passages. However, even at Passage 30, the viral titre of
626 compound **2**-treated cells remained lower than that of 0.1% DMSO-treated cells and
627 non-treated cells. We subjected the supernatant recovered from Passage 30 to dose-
628 dependent inhibition assay and unsurprisingly, compound **2** remains effective in
629 inhibiting the treated virus. As such, we believe that compound **2** is likely to be
630 targeting a host factor that prevents the virus from developing resistance.
631
632     We also investigated the potential for broad spectrum antiviral activity of
633 compound **2** against other enteroviruses. The viruses being investigated were CV-A16,
634 CV-A6 and EV-D68. We found that compound **2** was able to inhibit all three viruses
635 with $IC_{50}$ of 0.46 µM, 1.12 µM and 1.59 µM respectively. This was not a surprise as
636 earlier we speculate that compound **2** could be inhibiting a host factor involved in EV-
637 A71 RNA replication and the same host factor could be inhibited in the RNA replication
638 of these three viruses as the same cell line (RD) was used for infection. Nonetheless,
639 we do not rule out the possibility that compound **2** can act on multiple targets. Since
640 CV-A16 and CV-A6 are also responsible for causing HFMD among young children [60],
641 the discovery of compound **2** as a broad-spectrum antiviral agent can be further
642 explored to be use clinically as potential antiviral treatment against HFMD.
643
644     To date, the cellular targets of andro and its derivatives remained unclear. Hence,
645 while we speculate that compound **2** could be inhibiting a host factor involved in EV-
646 A71 RNA replication, more research is needed to identify the precise target. While
647 andro has been reported to target the p38 MAPK/Nrf2 and retinoic acid-inducible
648 gene-I (RIG-I)-like receptors (RLRs) signalling pathways for anti-HCV and anti-H1N1
649 activity respectively [16a,16b], targeting the NF-κB signalling pathway is a more
650 relevant antiviral approach with regard to EV-A71 infection since EV-A71 infection
651 activates NF-κB signalling which is crucial for viral replication and virus-induced
652 inflammatory responses [61] and andro is found to be a NF-κB inhibitor [26, 62].
653 However, our previous result [23c] shown that there NF-κB may not be taken as the
654 primary target of 8,17-epoxide andro analogs which suggests other existing targets of
655 inhibition triggered by the introduction of 8,17-epoxide. Andro is also reportedly
656 capable of inducing heme oxygenase 1 (HO-1) expression [63]. In relation to EV-A71
657 infection, it is shown that overexpression of HO-1 can inhibit EV-A71 replication and
658 EV-A71-induced NAPH oxidase activation and ROS generation which are responsible
659 for causing oxidative stress and the development of pathological conditions including
660 encephalitis [64]. However, it is unlikely that compound **2** exerts anti-EV-A71 activity
661 through HO-1 as it would have significantly inhibited EV-A71 infection in the pre-
662 treatment assay which was not the case. Nrf2 activation by covalently binding Keap1
663 of andro scaffold via Michael reaction is correlated with activation of HO-1 [27-30]. No
664 EV-A71 inhibition in the pre-treatment assay also likely to indicate no obvious HO-1
665 activation which suggests that at least compound **2** does not primarily behave as

Michael acceptor. Hence, we speculate that introduction of 8,17-epoxide makes compound **2** more likely to bind other target/s or/and a hindrance to approach double bond by Michael donor/s from NF-κB, Keap1 and etc. Further study for elucidation of action of mode is expected.

In summary, we discovered compound **2** of 14$S$-(2'-chloro-4'-nitrophenoxy)-8$R$/$S$,17-epoxy andrographolide as anti-EV-A71 infection agent by inhibiting the post-entry stages of EV-A71 viral replication cycle. Compound **2** significantly reduces viral titre and viral protein expression via inhibiting EV-A71 RNA replication. Meanwhile, compound **2** is likely to target a host factor in EV-A71 RNA replication and exert broad-spectrum antiviral effects against other enteroviruses. As a result, andrographolide scaffold mounted with 14-aryloxy and 8,17-epoxide moieties is a potential anti-EV-A71 strategy. Future work to discover more potent andrographolide derivatives, elucidate comprehensive SAR and understand the mechanism of drug action is under way.

**Authorship contribution statement**

**Guo-Chun Zhou:** Conceptualization, Data curation, Formal analysis, Funding acquisition, Project administration, Resources, Supervision, Writing – review & editing. **Justin Jang Hann Chu:** Conceptualization, Data curation, Formal analysis, Funding acquisition, Project administration, Resources, Supervision, Writing – review & editing. **Kun Dai:** Data curation, Formal analysis, Investigation, Methodology, Software, Validation, Writing – original draft. **Jie Kai Tan:** Data curation, Formal analysis, Investigation, Methodology, Software, Validation, Writing – original draft. **Weiyi Qian:** Data curation, Investigation, Software. **Regina Ching Hua Lee:** Data curation, Investigation, Software.

**Declaration of competing interest**

The authors declare that they have no known competing financial interests or personal relationships that could have appeared to influence the work reported in this paper.

**References**

[1] N.J. Schmidt, E.H. Lennette, H.H. Ho, An apparently new enterovirus isolated from patients with disease of the central nervous system, J Infect Dis 129(3) (1974) 304-9.
[2] M. Chumakov, M. Voroshilova, L. Shindarov, I. Lavrova, L. Gracheva, G. Koroleva, S. Vasilenko, I. Brodvarova, M. Nikolova, S. Gyurova, M. Gacheva, G. Mitov, N. Ninov, E. Tsylka, I. Robinson, M. Frolova, V. Bashkirtsev, L. Martiyanova, V. Rodin, Enterovirus 71 isolated from cases of epidemic poliomyelitis-like disease in Bulgaria, Arch Virol 60(3-4) (1979) 329-40.
[3] G. Nagy, S. Takatsy, E. Kukan, I. Mihaly, I. Domok, Virological diagnosis of enterovirus type 71 infections: experiences gained during an epidemic of acute CNS diseases in Hungary in 1978, Arch Virol 71(3) (1982) 217-27.

713  [4] J. Puenpa, N. Wanlapakorn, S. Vongpunsawad, Y. Poovorawan, The History of Enterovirus A71
714  Outbreaks and Molecular Epidemiology in the Asia-Pacific Region, J Biomed Sci 26(1) (2019) 75.
715  [5] B. Yang, F. Liu, Q. Liao, P. Wu, Z. Chang, J. Huang, L. Long, L. Luo, Y. Li, G.M. Leung, B.J. Cowling, H.
716  Yu, Epidemiology of hand, foot and mouth disease in China, 2008 to 2015 prior to the introduction of
717  EV-A71 vaccine, Euro Surveill 22(50) (2017).
718  [6] W.K. Phyu, K.C. Ong, K.T. Wong, Modelling person-to-person transmission in an Enterovirus A71
719  orally infected hamster model of hand-foot-and-mouth disease and encephalomyelitis, Emerg
720  Microbes Infect 6(7) (2017) e62.
721  [7] J. Yuan, L. Shen, J. Wu, X. Zou, J. Gu, J. Chen, L. Mao, Enterovirus A71 Proteins: Structure and
722  Function, Front Microbiol 9 (2018) 286.
723  [8] S.W. Huang, Y.H. Huang, H.P. Tsai, P.H. Kuo, S.M. Wang, C.C. Liu, J.R. Wang, A Selective Bottleneck
724  Shapes the Evolutionary Mutant Spectra of Enterovirus A71 during Viral Dissemination in Humans, J
725  Virol 91(23) (2017).
726  [9] M.H. Ooi, S.C. Wong, P. Lewthwaite, M.J. Cardosa, T. Solomon, Clinical features, diagnosis, and
727  management of enterovirus 71, Lancet Neurol 9(11) (2010) 1097-105.
728  [10] S. Esposito, N. Principi, Hand, foot and mouth disease: current knowledge on clinical
729  manifestations, epidemiology, aetiology and prevention, Eur J Clin Microbiol Infect Dis 37(3) (2018)
730  391-398.
731  [11] Z.H. Li, C.M. Li, P. Ling, F.H. Shen, S.H. Chen, C.C. Liu, C.K. Yu, S.H. Chen, Ribavirin reduces mortality
732  in enterovirus 71-infected mice by decreasing viral replication, J Infect Dis 197(6) (2008) 854-7.
733  [12] T.Y. Lin, C. Chu, C.H. Chiu, Lactoferrin inhibits enterovirus 71 infection of human embryonal
734  rhabdomyosarcoma cells in vitro, J Infect Dis 186(8) (2002) 1161-4.
735  [13] G. Zhang, F. Zhou, B. Gu, C. Ding, D. Feng, F. Xie, J. Wang, C. Zhang, Q. Cao, Y. Deng, W. Hu, K. Yao,
736  In vitro and in vivo evaluation of ribavirin and pleconaril antiviral activity against enterovirus 71
737  infection, Arch Virol 157(4) (2012) 669-79.
738  [14] J.N. Wang, C.T. Yao, C.N. Yeh, C.C. Huang, S.M. Wang, C.C. Liu, J.M. Wu, Critical management in
739  patients with severe enterovirus 71 infection, Pediatr Int 48(3) (2006) 250-6.
740  [15] P.C. McMinn, An overview of the evolution of enterovirus 71 and its clinical and public health
741  significance, FEMS Microbiol Rev 26(1) (2002) 91-107.
742  [16] M.K. Gorter, The bitter constituent of Andrographis paniculata, 30 (1911) 151-160.
743  [17] R.J.C. Kleipool, Constituents of Andrographis paniculata Nees, Nature 169 (1952) 33-34.
744  [18] W.R.C. M.P. Cava, L.J. Haynes, L.F .Johnson, B. Weinstein, The structure of andrographolide,
745  Tetrahedron 18(4) (1962) 397-403.
746  [19] W.L. Deng, J.Y. Liu, R.J. Nie, [Pharmacological studies on 14-deoxy-11, 12-
747  didehydroandrographolide-3, 19-disuccinate. I. Anti-inflammatory activity (author's transl)], Yao Xue
748  Xue Bao 15(10) (1980) 590-7.
749  [20] T. Zhang, [Advances in the study of Andrographis paniculata (Burm.f.) Nees], Zhong Yao Cai 23(6)
750  (2000) 366-8.
751  [21] X. Liu, Y. Wang, G. Li, [Advances in pharmacological study of andrographolide and its derivatives],
752  Zhong Yao Cai 26(2) (2003) 135-8.
753  [22] S. Hossain, Z. Urbi, H. Karuniawati, R.B. Mohiuddin, A. Moh Qrimida, A.M.M. Allzrag, L.C. Ming, E.
754  Pagano, R. Capasso, Andrographis paniculata (Burm. f.) Wall. ex Nees: An Updated Review of
755  Phytochemistry, Antimicrobial Pharmacology, and Clinical Safety and Efficacy, Life (Basel) 11(4) (2021).
756  [23] A.K. Jadhav, S.M. Karuppayil, Andrographis paniculata (Burm. F) Wall ex Nees: Antiviral properties,
757  Phytother Res 35(10) (2021) 5365-5373.
758  [24] M. Jiang, F. Sheng, Z. Zhang, X. Ma, T. Gao, C. Fu, P. Li, Andrographis paniculata (Burm.f.) Nees
759  and its major constituent andrographolide as potential antiviral agents, J Ethnopharmacol 272 (2021)
760  113954.
761  [25] S. Kumar, B. Singh, V. Bajpai, Andrographis paniculata (Burm.f.) Nees: Traditional uses,
762  phytochemistry, pharmacological properties and quality control/quality assurance, J Ethnopharmacol
763  275 (2021) 114054.

764 [26] Y.F. Xia, B.Q. Ye, Y.D. Li, J.G. Wang, X.J. He, X. Lin, X. Yao, D. Ma, A. Slungaard, R.P. Hebbel, N.S.
765 Key, J.G. Geng, Andrographolide attenuates inflammation by inhibition of NF-kappa B activation
766 through covalent modification of reduced cysteine 62 of p50, J Immunol 173(6) (2004) 4207-17.
767 [27] J.C. Lee, C.K. Tseng, K.C. Young, H.Y. Sun, S.W. Wang, W.C. Chen, C.K. Lin, Y.H. Wu,
768 Andrographolide exerts anti-hepatitis C virus activity by up-regulating haeme oxygenase-1 via the p38
769 MAPK/Nrf2 pathway in human hepatoma cells, Br J Pharmacol 171(1) (2014) 237-52.
770 [28] B. Yu, C.Q. Dai, Z.Y. Jiang, E.Q. Li, C. Chen, X.L. Wu, J. Chen, Q. Liu, C.L. Zhao, J.X. He, D.H. Ju, X.Y.
771 Chen, Andrographolide as an anti-H1N1 drug and the mechanism related to retinoic acid-inducible
772 gene-I-like receptors signaling pathway, Chin J Integr Med 20(7) (2014) 540-5.
773 [29] S.Y. Wong, M.G. Tan, P.T. Wong, D.R. Herr, M.K. Lai, Andrographolide induces Nrf2 and heme
774 oxygenase 1 in astrocytes by activating p38 MAPK and ERK, J Neuroinflammation 13(1) (2016) 251.
775 [30] T.L. Yen, R.J. Chen, T. Jayakumar, W.J. Lu, C.Y. Hsieh, M.J. Hsu, C.H. Yang, C.C. Chang, Y.K. Lin, K.H.
776 Lin, J.R. Sheu, Andrographolide stimulates p38 mitogen-activated protein kinase-nuclear factor
777 erythroid-2-related factor 2-heme oxygenase 1 signaling in primary cerebral endothelial cells for
778 definite protection against ischemic stroke in rats, Transl Res 170 (2016) 57-72.
779 [31] R. Latif, C.Y. Wang, Andrographolide as a potent and promising antiviral agent, Chin J Nat Med
780 18(10) (2020) 760-769.
781 [32] S. Gupta, K.P. Mishra, L. Ganju, Broad-spectrum antiviral properties of andrographolide, Arch Virol
782 162(3) (2017) 611-623.
783 [33] L. Ye, T. Wang, L. Tang, W. Liu, Z. Yang, J. Zhou, Z. Zheng, Z. Cai, M. Hu, Z. Liu, Poor oral
784 bioavailability of a promising anticancer agent andrographolide is due to extensive metabolism and
785 efflux by P-glycoprotein, J Pharm Sci 100(11) (2011) 5007-17.
786 [34] M. Hao, M. Lv, H. Xu, Andrographolide: Synthetic Methods and Biological Activities, Mini Rev Med
787 Chem 20(16) (2020) 1633-1652.
788 [35] G. Kumar, D. Singh, J.A. Tali, D. Dheer, R. Shankar, Andrographolide: Chemical modification and
789 its effect on biological activities, Bioorg Chem 95 (2020) 103511.
790 [36] V. Kishore, N.S. Yarla, A. Bishayee, S. Putta, R. Malla, N.R. Neelapu, S. Challa, S. Das, Y. Shiralgi, G.
791 Hegde, B.L. Dhananjaya, Multi-targeting Andrographolide and its Natural Analogs as Potential
792 Therapeutic Agents, Curr Top Med Chem 17(8) (2017) 845-857.
793 [37] Y.Y. Yan, G.X. Shi, J. Shao, T.M. Wang, C.Z. Wang, [Advance in studies on anti-infection of
794 andrographolide and its derivatives in past 10 years], Zhongguo Zhong Yao Za Zhi 38(22) (2013) 3819-
795 24.
796 [38] C.P. Commission, Chuanhuning (article in Chinese), Chin. Pharmacop. 2 (2010) 619-620.
797 [39] A. Basak, S. Cooper, A.G. Roberge, U.K. Banik, M. Chretien, N.G. Seidah, Inhibition of proprotein
798 convertases-1, -7 and furin by diterpines of Andrographis paniculata and their succinoyl esters,
799 Biochem J 338 ( Pt 1)(Pt 1) (1999) 107-13.
800 [40] R.S. Chang, L. Ding, G.Q. Chen, Q.C. Pan, Z.L. Zhao, K.M. Smith, Dehydroandrographolide succinic
801 acid monoester as an inhibitor against the human immunodeficiency virus, Proc Soc Exp Biol Med
802 197(1) (1991) 59-66.
803 [41] M. Li, X. Yang, C. Guan, T. Wen, Y. Duan, W. Zhang, X. Li, Y. Wang, Z. Zhao, S. Liu, Andrographolide
804 sulfonate reduces mortality in Enterovirus 71 infected mice by modulating immunity, Int
805 Immunopharmacol 55 (2018) 142-150.
806 [42] X. Li, C. Zhang, Q. Shi, T. Yang, Q. Zhu, Y. Tian, C. Lu, Z. Zhang, Z. Jiang, H. Zhou, X. Wen, H. Yang,
807 X. Ding, L. Liang, Y. Liu, Y. Wang, A. Lu, Improving the efficacy of conventional therapy by adding
808 andrographolide sulfonate in the treatment of severe hand, foot, and mouth disease: a randomized
809 controlled trial, Evid Based Complement Alternat Med 2013 (2013) 316250.
810 [43] T. Wen, W. Xu, L. Liang, J. Li, X. Ding, X. Chen, J. Hu, A. Lv, X. Li, Clinical Efficacy of Andrographolide
811 Sulfonate in the Treatment of Severe Hand, Foot, and Mouth Disease (HFMD) is Dependent upon
812 Inhibition of Neutrophil Activation, Phytother Res 29(8) (2015) 1161-7.

813 [44] W.-K.L. Z. Liu, D. Wang, X. Nie, D. Sheng, G. Song, K. Guo, P. Wei, P. Ouyang, C.-W. Wong, G.-C.
814 Zhou, Synthesis and discovery of andrographolide derivatives as non-steroidal farnesoid X receptor
815 (FXR) antagonists, RSC Adv 4 (2014) 13533-13545.
816 [45] J. Li, Y. Peng, S. Li, Y. Sun, J.Y. Chan, G. Cui, D. Wang, G.C. Zhou, S.M. Lee, Anti-angiogenic activity
817 of a new andrographolide derivative in zebrafish and HUVECs, Eur J Pharmacol 789 (2016) 344-353.
818 [46] F. Li, W. Khanom, X. Sun, A. Paemanee, S. Roytrakul, D. Wang, D.R. Smith, G.C. Zhou,
819 Andrographolide and Its 14-Aryloxy Analogues Inhibit Zika and Dengue Virus Infection, Molecules
820 25(21) (2020).
821 [47] F. Li, E.M. Lee, X. Sun, D. Wang, H. Tang, G.C. Zhou, Design, synthesis and discovery of
822 andrographolide derivatives against Zika virus infection, Eur J Med Chem 187 (2020) 111925.
823 [48] H.W. Xu, G.F. Dai, G.Z. Liu, J.F. Wang, H.M. Liu, Synthesis of andrographolide derivatives: a new
824 family of alpha-glucosidase inhibitors, Bioorg Med Chem 15(12) (2007) 4247-55.
825 [49] R. Preet, B. Chakraborty, S. Siddharth, P. Mohapatra, D. Das, S.R. Satapathy, S. Das, N.C. Maiti,
826 P.R. Maulik, C.N. Kundu, C. Chowdhury, Synthesis and biological evaluation of andrographolide
827 analogues as anti-cancer agents, Eur J Med Chem 85 (2014) 95-106.
828 [50] S.R. Chen, F. Li, M.Y. Ding, D. Wang, Q. Zhao, Y. Wang, G.C. Zhou, Y. Wang, Andrographolide
829 derivative as STAT3 inhibitor that protects acute liver damage in mice, Bioorg Med Chem 26(18) (2018)
830 5053-5061.
831 [51] K.X. Wu, J.J. Chu, Antiviral screen identifies EV71 inhibitors and reveals camptothecin-target, DNA
832 topoisomerase 1 as a novel EV71 host factor, Antiviral Res 143 (2017) 122-133.
833 [52] J. Lu, Y.Q. He, L.N. Yi, H. Zan, H.F. Kung, M.L. He, Viral kinetics of enterovirus 71 in human
834 abdomyosarcoma cells, World J Gastroenterol 17(36) (2011) 4135-42.
835 [53] C.C. Liu, M.S. Guo, F.H. Lin, K.N. Hsiao, K.H. Chang, A.H. Chou, Y.C. Wang, Y.C. Chen, C.S. Yang, P.C.
836 Chong, Purification and characterization of enterovirus 71 viral particles produced from vero cells
837 grown in a serum-free microcarrier bioreactor system, PLoS One 6(5) (2011) e20005.
838 [54] S. Gunaseelan, K.Z. Wong, N. Min, J. Sun, N. Ismail, Y.J. Tan, R.C.H. Lee, J.J.H. Chu, Prunin
839 suppresses viral IRES activity and is a potential candidate for treating enterovirus A71 infection, Sci
840 Transl Med 11(516) (2019).
841 [55] X. Lv, M. Qiu, D. Chen, N. Zheng, Y. Jin, Z. Wu, Apigenin inhibits enterovirus 71 replication through
842 suppressing viral IRES activity and modulating cellular JNK pathway, Antiviral Res 109 (2014) 30-41.
843 [56] G. Zhang, Y. Hou, Y. Li, L. He, L. Tang, T. Yang, X. Zou, Q. Zhu, S. Yan, B. Huang, J. Zhao, J. Huang,
844 Xiyanping injection therapy for children with mild hand foot and mouth disease: a randomized
845 controlled trial, J Tradit Chin Med 37(3) (2017) 397-403.
846 [57] D. Wang, H. Guo, J. Chang, D. Wang, B. Liu, P. Gao, W. Wei, Andrographolide Prevents EV-D68
847 Replication by Inhibiting the Acidification of Virus-Containing Endocytic Vesicles, Front Microbiol 9
848 (2018) 2407.
849 [58] K.E. Murray, M.L. Nibert, Guanidine hydrochloride inhibits mammalian orthoreovirus growth by
850 reversibly blocking the synthesis of double-stranded RNA, J Virol 81(9) (2007) 4572-84.
851 [59] T. Schneider-Poetsch, J. Ju, D.E. Eyler, Y. Dang, S. Bhat, W.C. Merrick, R. Green, B. Shen, J.O. Liu,
852 Inhibition of eukaryotic translation elongation by cycloheximide and lactimidomycin, Nat Chem Biol
853 6(3) (2010) 209-217.
854 [60] L.W. Ang, J. Tay, M.C. Phoon, J.P. Hsu, J. Cutter, L. James, K.T. Goh, V.T. Chow, Seroepidemiology
855 of Coxsackievirus A6, Coxsackievirus A16, and Enterovirus 71 Infections among Children and
856 Adolescents in Singapore, 2008-2010, PLoS One 10(5) (2015) e0127999.
857 [61] Y. Jin, R. Zhang, W. Wu, G. Duan, Antiviral and Inflammatory Cellular Signaling Associated with
858 Enterovirus 71 Infection, Viruses 10(4) (2018).
859 [62] C.C. Chang, Y.F. Duann, T.L. Yen, Y.Y. Chen, T. Jayakumar, E.T. Ong, J.R. Sheu, Andrographolide, a
860 Novel NF-kappaB Inhibitor, Inhibits Vascular Smooth Muscle Cell Proliferation and Cerebral
861 Endothelial Cell Inflammation, Acta Cardiol Sin 30(4) (2014) 308-15.

862    [63] A.L. Yu, C.Y. Lu, T.S. Wang, C.W. Tsai, K.L. Liu, Y.P. Cheng, H.C. Chang, C.K. Lii, H.W. Chen, Induction
863    of heme oxygenase 1 and inhibition of tumor necrosis factor alpha-induced intercellular adhesion
864    molecule expression by andrographolide in EA.hy926 cells, J Agric Food Chem 58(13) (2010) 7641-8.
865    [64] W.H. Tung, H.L. Hsieh, I.T. Lee, C.M. Yang, Enterovirus 71 induces integrin beta1/EGFR-Rac1-
866    dependent oxidative stress in SK-N-SH cells: role of HO-1/CO in viral replication, J Cell Physiol 226(12)
867    (2011) 3316-29.

868
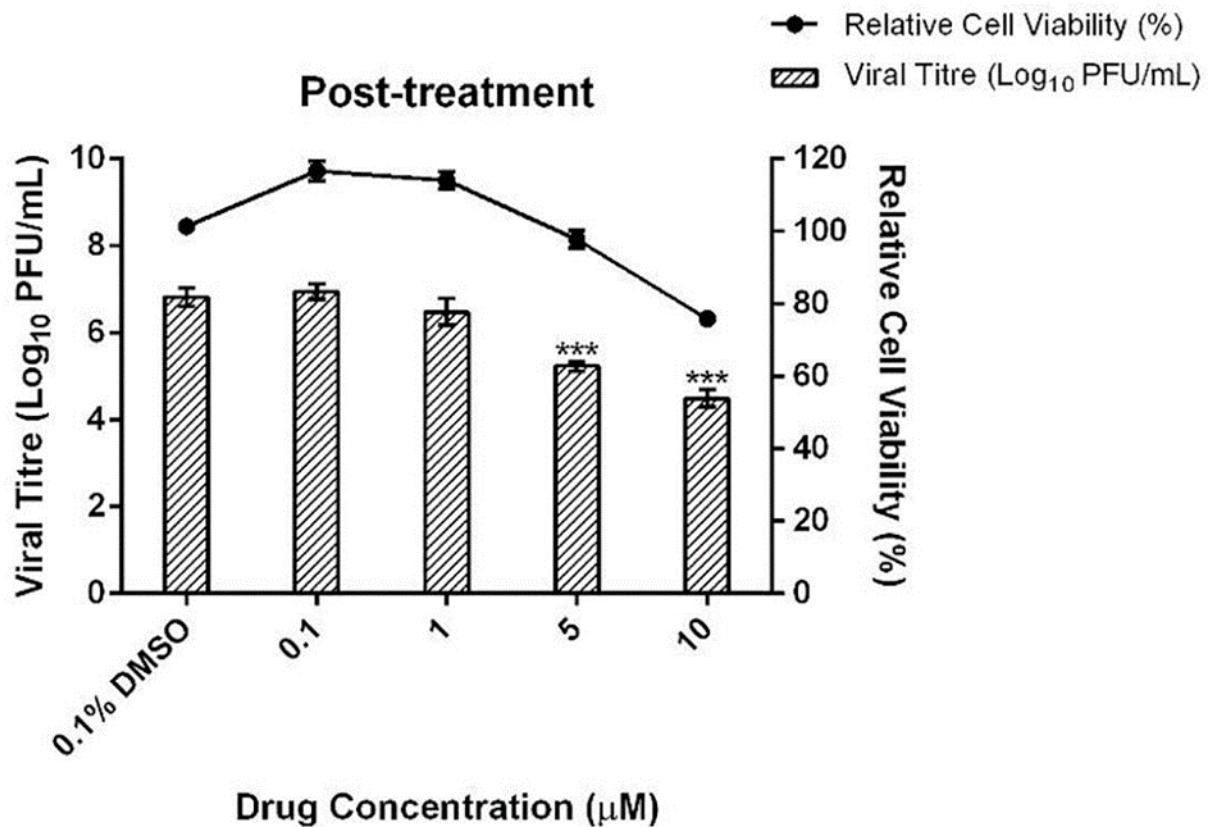
**Fig. 1. Cytotoxicity, anti-EV-A71 activity and viral titre of compound 2.** EV-A71-infected RD cells were treated with compound **2** at various concentrations and significant viral reductions were observed (shown in Table 1). The left y-axis measures the viral titre while the right y-axis measures the relative cell viability. Each data point/bar indicates the mean of triplicates and error bars signify their standard deviation. Statistical analyses were accomplished using one-way ANOVA and Dunnett's post-test. *** indicates $p < 0.001$.
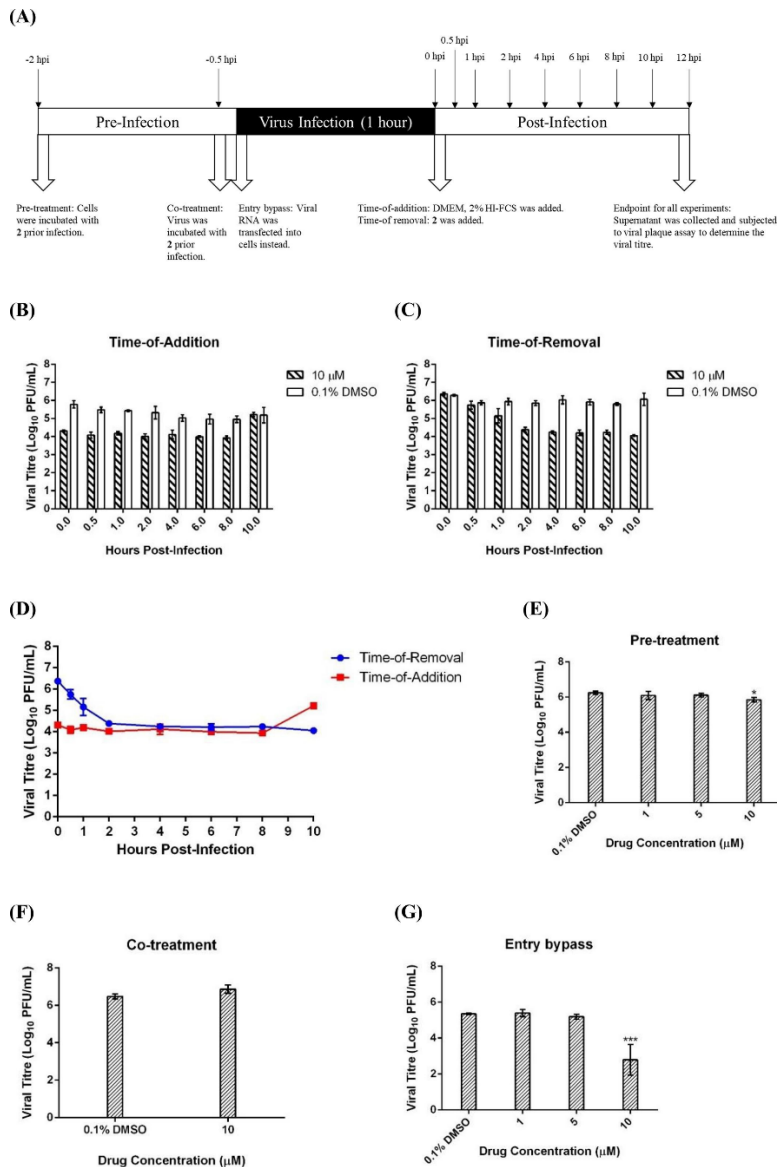
**Fig. 2. Compound 2 inhibits the post-entry stages of EV-A71 viral replication cycle. (A)** Schematic illustration of the process of time point dependent assays. **(B)** Time-of-addition assay comparing 10 µM of compound **2** with 0.1% DMSO. **(C)** Time-of-removal assay comparing 10 µM of compound **2** with 0.1% DMSO. **(D)** Combined results of both time-of-addition and time-of-removal assays for 10 µM of compound **2**. **(E)** Pre-treatment with compound **2** showed significant viral reduction at the highest concentration used although the reduction was not as pronounced as treatment post-infection. Viral titres at other concentrations remained similar to 0.1% DMSO suggest that compound **2** is unlikely to inhibit EV-A71 entry into host cells. **(F)** Co-treatment with compound **2** showed no significant difference in viral titres suggests that compound **2** is unlikely to interact with viral surface proteins to inhibit viral entry. **(G)** Entry bypass assay showed significant viral reduction for EV-A71 RNA transfected cells treated with compound **2** at 10 µM, suggesting that compound **2** is likely to inhibit the late stages of EV-A71 replication. Each data point/bar indicates the mean of triplicates and error bars signify their standard deviation. Statistical analyses were accomplished using one-way ANOVA and Dunnett's post-test. ** indicates $p < 0.01$ and *** indicates $p < 0.001$.

896
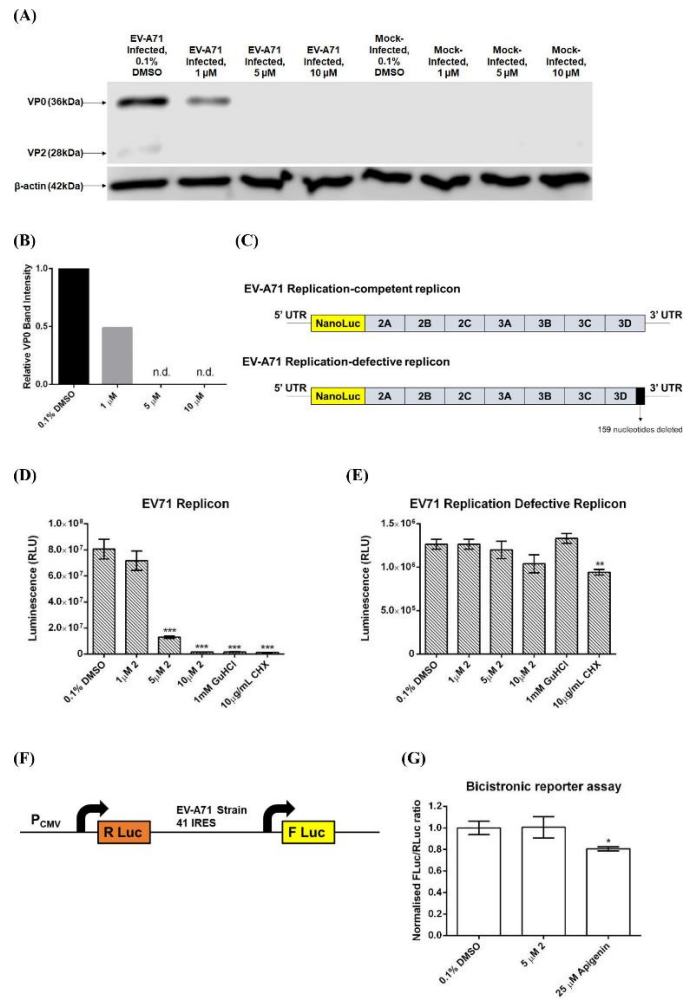
**Fig. 3. Compound 2 reduces viral protein expression by inhibiting EV-A71 RNA replication. (A)** Western blot detection showed significant dose-dependent reductions in VP2 and VP0 band intensities at 6 hpi upon treatment with compound **2** suggests that compound **2** can affect viral protein synthesis in host cells. **(B)** Relative band intensity of VP0 was obtained by comparing samples treated with compound **2** with 0.1% DMSO. **(C)** EV-A71 replication-competent and replication-defective replicons used in nano-luciferase reporter assay. **(D)** Nano-luciferase reporter assay on RD cells transfected with replication-competent replicon. Treatment with compound **2** led to significant dose-dependent reduction in luminescence. **(E)** Nano-luciferase reporter assay on RD cells transfected with replication-defective replicon. No significant dose-dependent reduction in luminescence was observed. This suggests that compound **2** inhibits EV-A71 RNA replication but not IRES-mediated protein translation. GuHCl and CHX serve as positive controls. **(F)** Bicistronic reporter construct used in bicistronic luciferase reporter assay. **(G)** Bicistronic reporter assay on RD cells transfected with bicistronic reporter construct. IRES-mediated translation activity was represented by FLuc/RLuc. Treatment with compound **2** did not affect IRES activity. Apigenin serves as positive control. Each bar indicates the mean of triplicates and error bars signify their standard deviation. Statistical analyses were accomplished using one-way ANOVA and Dunnett's post-test. * indicates $p < 0.05$, ** indicates $p < 0.01$ and *** indicates $p < 0.001$.

**(A)**



**(B)**
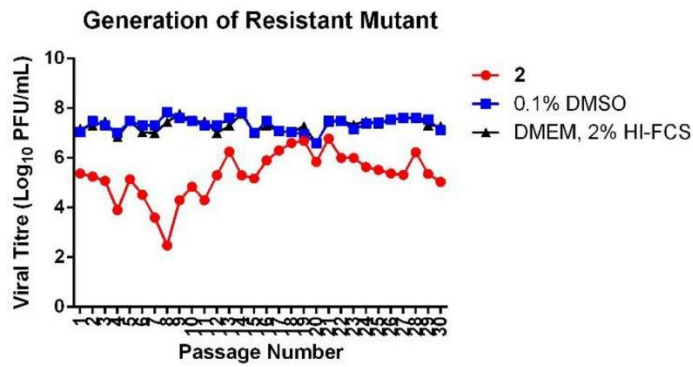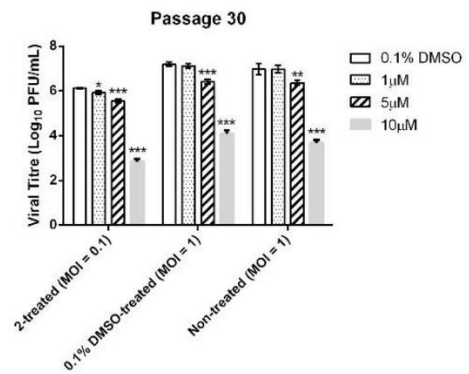


**Fig. 4. Attempts to generate EV-A71 resistant mutants against compound 2.**
**(A)** Viral titres at every passage correspond to treatment with compound **2** (red), 0.1% DMSO (blue) and DMEM, 2% HI-FCS (black). At 12 hpi, the supernatant was recovered and used to infect a subsequent passage. From Passage 1 to 20, 5 µM of compound **2** was used. From Passage 21–30, 7.5 µM of compound **2** was used. **(B)** Dose-dependent inhibition assay performed on supernatant harvested from Passage 30. Significant reductions in viral titre were observed after treatment with compound **2** in a dose-dependent manner suggests that no resistance has been developed yet. Each data point/bar indicates the mean of triplicates and error bars signify their standard deviation. Statistical analyses were accomplished using one-way ANOVA and Dunnett's post-test. * indicates $p < 0.05$, ** indicates $p < 0.01$ and *** indicates $p < 0.001$. (For interpretation of the references to colour in this figure legend, the reader is referred to the web version of this article.)

**(A) CV-A16**
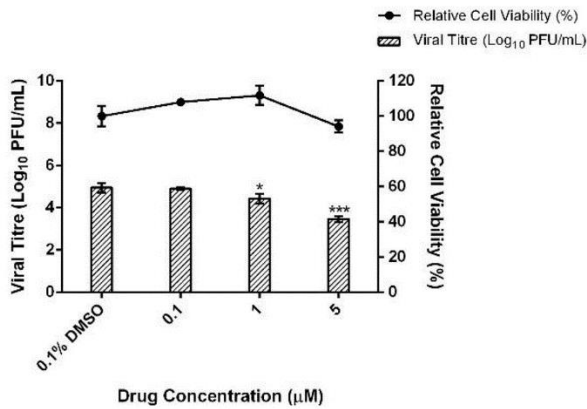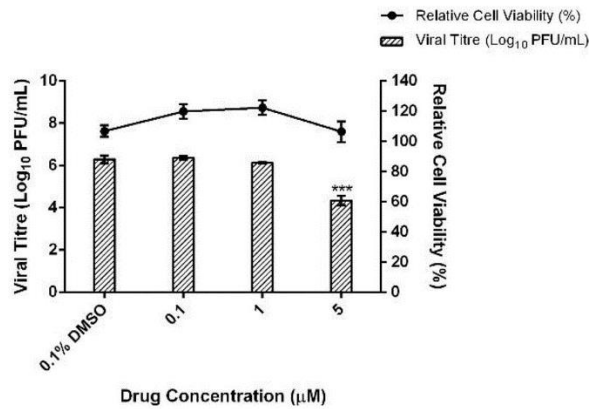


**(B) CV-A6**



**(C) EV-D68**
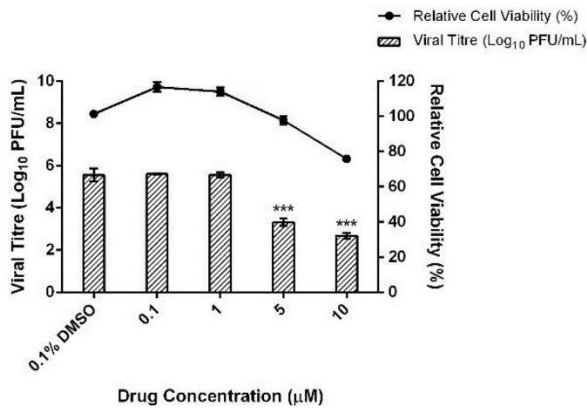


**Fig. 5. Antiviral effects of compound 2 on other enteroviruses. (A)** CV-A16, **(B)** CV-A6 and **(C)** EV-D68 -infected RD cells were treated with compound **2** at various concentrations and viral titre was ascertained with viral plaque assay. Significant reduction in viral titres were observed for all enteroviruses upon treatment with compound **2**. The left y-axis measures the viral titre while the right y-axis measures the relative cell viability. Each data point/bar indicates the mean of triplicates and error bars signify their standard deviation. Statistical analyses were accomplished using one-way ANOVA and Dunnett's post-test. ** indicates $p < 0.01$ and *** indicates $p < 0.001$.
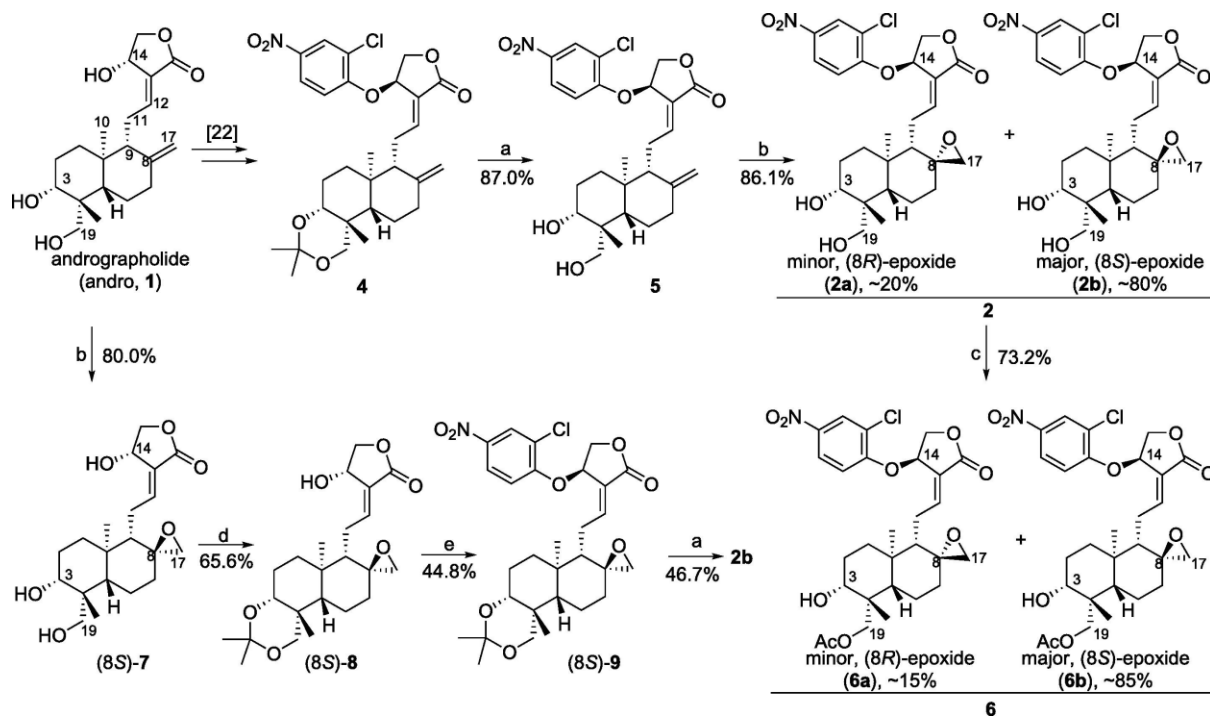
946

947 **Scheme 1.** Reagents and conditions: (a) TsOH·H$_2$O, MeOH, room temperature,
948 30 min. (b) mCPBA, NaHCO$_3$, DCM, room temperature, 12 h. (c) AcCl, TEA, DCM,
949 0 °C, 5 h. (d) 2,2-dimethoxypropane, PPTS, DCM, 45 °C, 3 h. (e) 2-Chloro-4-
950 nitrophenol, PPh$_3$, DIAD, THF, 0 °C, 2 h.

951

952   **Table 1.** Values of viral titre reduction, $CC_{50}$, $IC_{50}$ and SI of compounds 2, 2b and 6.

953

| Compound | Log$_{10}$ PFU/mL viral titre reduction at | | $CC_{50}$ (µM) | $IC_{50}$ (µM) | Selectivity Index (SI) |
|---|---|---|---|---|---|
| | **5 µM** | **10 µM** | | | |
| **2** | 1.60 | 2.30 | 11.64 | 0.95 | 12.28 |
| **2b** | 0.61 | 1.41 | 14.42 | /[a] | /[a] |
| **6** | 0.63 | 2.27 | 10.50 | /[a] | /[a] |

954   [a]Not available.

955

956   **Table 2.** $IC_{50}$ values of 2 against other Enteroviruses.

957

| Enterovirus | Species | Drug treatment duration (h) | $IC_{50}$ (µM) |
|---|---|---|---|
| CV-A16 | Enterovirus A | 16 | 0.46 |
| CV-A6 | Enterovirus A | 96 | 1.12 |
| EV-D68 | Enterovirus D | 12 | 1.59 |

958